Scour-monitoring techniques for offshore foundations

Yong-Hoon Byun[a], Kiwon Park[b] and Jong-Sub Lee[*]

*School of Civil, Environmental and Architectural Engineering, Korea University, 145, Anam-ro,
Sungbuk-gu, Seoul, 136-713, Korea*

Abstract.   The scour induced by strong currents and wave action decreases the embedded length of monopiles and leads to a decrease of their structural stability. The objective of this study is the development and consideration of scour-monitoring techniques for offshore monopile foundations. Tests on physical models are carried out with a model monopile and geo-materials prepared in a cylindrical tank. A strain gauge, two coupled ultrasonic transducers, and ten electrodes are used for monitoring the scour. The natural frequency, ultrasonic reflection images, and electrical resistivity profiles are obtained at various scour depths. The experimental results show that the natural frequency of the model monopile decreases with an increase in the scour depth and that the ultrasonic reflection images clearly detect the scour shape and scour depth. In addition, the electrical resistivity decreases with an increase in scour depth. This study suggests that natural frequency measurement, ultrasonic reflection imaging, and electrical resistivity profiling may be used as effective tools to monitor the scour around an offshore monopile foundation.

Keywords: electrical resistivity; monopole; natural frequency; scour depth; ultrasonic reflection

1. Introduction

Monopiles, which are used for supporting offshore wind turbines, have been recognized as a cost-effective foundation in water depths of less than 30 m (Andersen *et al*. 2012). However, at these offshore foundations, scour can be induced by strong currents and wave action, particularly in shallower water. The development of scour is dependent on the force imposed by the shear stress on soil particles and the weight of these soil particles submerged in water. Scour development leads to a decrease in the embedded length of a monopile. Eventually, the scour can cause damage to the cables that operate the turbines and decrease the structural stability. Thus, scour should be evaluated for offshore wind farms.

The prediction of scour around offshore foundations has been studied (Qi and Gao 2014, Zanke *et al*. 2011, Zhao *et al*. 2010). Den Boon *et al*. (2004) showed that, in a model test, the average maximum depth of scour corresponded to 1.75 times the pile diameter. Whitehouse *et al*. (2006, 2008) considered the maximum scour depth, the radial bed profiles, and the timescale of equilibrium scour, using model tests. Furthermore, the stability of scour protection was

---

∗Corresponding author, Professor, E-mail: jongsub@korea.ac.kr
[a] Postdoctoral Fellow
[b] Graduate Student

investigated for the appropriate design and performance of the monopile. However, the precise prediction of scour is still difficult because scour development is strongly dependent on the site conditions.

Several techniques for monitoring scour around offshore foundations have been proposed by many researchers (Andrews and Bennett 1981, Babu *et al.* 2003, De Vries *et al.* 2001, Nawa and Frissell 1993). Cooper *et al.* (2000) applied a magnetic sliding collar device and a sonar device to monitor scour, even though the devices were not robust enough for long-term survivability. In addition, fiber Bragg grating sensors were effectively used for monitoring scour (Lin *et al.* 2006, Zhou *et al.* 2011). Briaud *et al.* (2012) proposed a new electrical resistivity survey method as a geophysical technique for the determination of scour. However, in the electrical resistivity survey method, the spacing and number of the electrodes should be considered in terms of their penetration depth and resolution. Furthermore, in the case of an offshore wind farm, the electrical resistivity survey is subject to limited access to the monopile foundation. These methods for monitoring scour still have a high level of uncertainty when applied to offshore foundations.

This study considers the natural frequency, ultrasonic reflection, and electrical resistivity for evaluating the scour around offshore monopile foundations. First, the monopile and geo-materials used for the physical model test are introduced. Then, this paper provides three different monitoring techniques, including the principle, the measurement system, and test results. Finally, the results of a physical model test for the application of these scour monitoring techniques are discussed.

2. Experimental setup

Scour around offshore foundations was simulated by using a model monopile and geo-materials in a cylindrical tank. According to the scour, the natural frequency of the monopile, the scour shape, and the scour depth were monitored by three different methods.

2.1 Model monopile

The model monopile was designed as a cylindrical pipe made with polyurethane (PPG type, P-90), as shown in Fig. 1. The model monopile has a height of 450 mm and a diameter of 25 mm. The cylindrical tank, which has a height of 400 mm and a diameter of 1000 mm, was used to contain the model ground with geo-materials. To simulate the monopile embedded in rock, the model monopile was fixed in the center of the bottom of cylindrical tank.

2.2 Geo-materials

For the simulation of the seabed, the model ground was prepared in a cylindrical tank after mixing Jumunjin sand and Portland cement. The sands and cement have a median grain size (D_{50}) of 0.36 mm and 0.02 mm, and the specific gravity of 2.62 and 3.15, respectively. The sands and cement were mixed in a ratio of 10 to 1 by weight, and then, the monopile was embedded in the lightly cemented soils. The scour depth was changed with a depth of 0, 50, 90, 110, and 130 mm, while the scour slope with an angle of 39° remained constant.
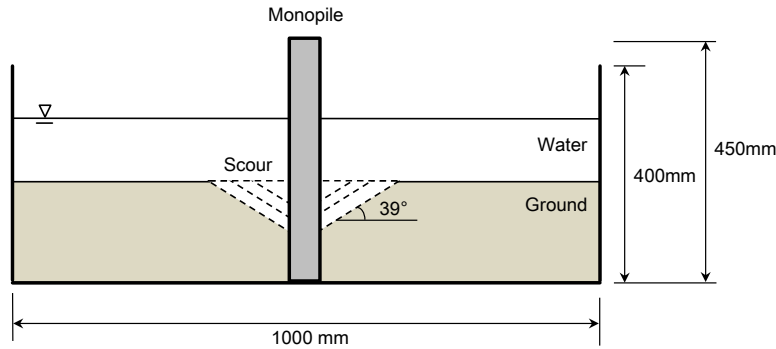
Fig. 1 Schematic drawing of the model monopile and ground prepared in a cylindrical tank

3. Natural frequency measurement

3.1 Principle

The scour causes a reduction of the embedded length of a monopile, resulting in a change in the natural frequency of the monopile. For the fixed-free-boundary condition, the natural frequency (f_n) of the pile can be expressed as follows (Meirovitch 1967, Lee and Santamarina 2005)

$$f_n = \frac{1}{2\pi}\sqrt{\frac{k_p}{m_p}} = \frac{1}{2\pi}\sqrt{\frac{1.875^4 E_p I}{\bar{m}(\alpha L_p)^4}} \tag{1}$$

where k_p, m_p, and E_p, are the equivalent spring constant, the pile mass, and the elastic modulus, respectively. I is the moment of inertia, which depends on the shape of the pile. L_p is the length of a pile, and the effective pile length (αL_p) can be determined by the selection of the value of α. For the rigid boundary condition, the value of α is set to be 1, and for the loose boundary condition, less than 1. Based on Eq. (1), the natural frequency of the monopile embedded in seabed and rock will decrease with an increase in the scour depth and the value of α will be greater than 1. The calculated natural frequency for the model monopile with a height of 450 mm is 26.8 Hz. In practice, however, the real natural frequency for the monopile may not be matched with the calculated natural frequency because of the environmental noise and the damping effect of water. Thus, in this study, as an alternative to the evaluation of the natural frequency by a determination of α, an experimental method using a strain gauge is proposed.

3.2 Measurement system

A strain gauge, which can convert mechanical resistance to a change in electrical resistance, was used to measure the natural frequency of the model monopile. The strain gauge was attached to the model monopile, as shown in Fig. 2. The strain gauge was connected to a data logger through the interface module. Lateral loading by the impact of a hammer was applied to the top of the model monopile. The natural frequency of the model monopile was then recorded in the data logger, which adjusted the low pass filter in a range from 10 to 1,000 Hz.
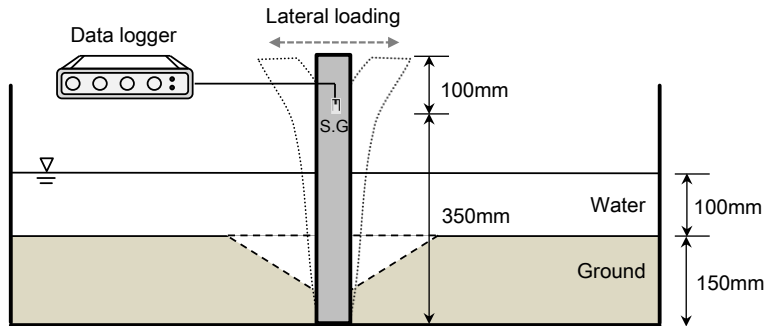
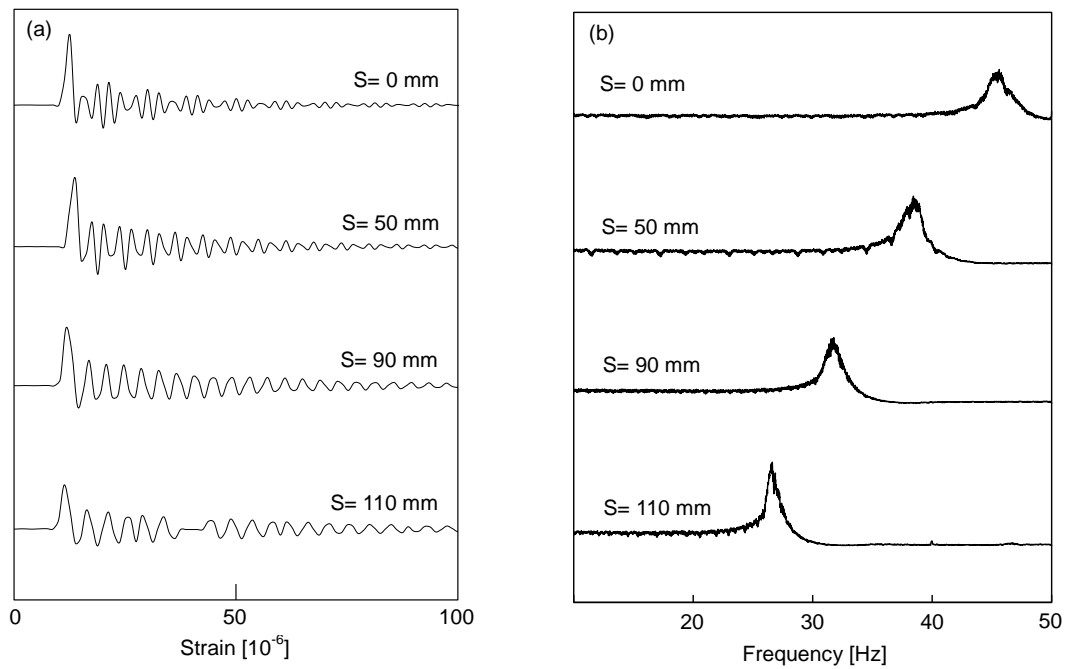Fig. 2 Measurement system for a dynamic response using a strain gauge

Fig. 3 Dynamic responses: (a) time domain and (b) frequency domain. S denotes the scour depth

3.3 Test results

Dynamic strain signals of the model monopile were obtained from the strain gauge in order to evaluate the natural frequency. In the model test, the scour depths were set to 0, 50, 90, and 110 mm. The variation of dynamic strain signals according to the scour depth is plotted in Fig. 3(a). Provided that a constant energy from the impact of the hammer was transferred to the model monopile, the duration of the signal increased with an increase in the scour depth. To determine the natural frequency of the model monopile, fast Fourier transform (FFT) was used, which is an

algorithm to convert time to frequency. Fig. 3(b) shows the variation in the spectrum of dynamic strain signals according to the scour depth. For a scour depth of 0 mm, the natural frequency of the model monopile is 46.0 Hz, and for a scour depth of 110 mm, the natural frequency is 27.8 Hz. The results demonstrate that the natural frequency of the model monopile decreases with an increase in the scour depth.

4. Ultrasonic reflection imaging

4.1 Principle

The ultrasonic wave reflection method is based on monitoring compressional waves (greater than 20 kHz) reflected from an interface defined as the boundary between two media. As the compressional waves travel through the medium with different acoustic impedances, some waves are reflected and others continue to propagate forward. The coefficients of reflection and transmission describe the amount of wave energy, which is reflected and transmitted at the interface, respectively. In the case of normal incidence, the coefficients of reflection (R) and transmission (T) can be determined by the acoustic impedances (z_1 and z_2) of any two media as follows.

$$\text{Reflection coefficient:} \quad R = \frac{Z_2 - Z_1}{Z_2 + Z_1} = \frac{\rho_2 V_2 - \rho_1 V_1}{\rho_2 V_2 + \rho_1 V_1} \tag{2}$$

$$\text{Transmission coefficient:} \quad T = \frac{2Z_2}{Z_2 + Z_1} = \frac{2\rho_2 V_2}{\rho_2 V_2 + \rho_1 V_1} \tag{3}$$

where ρ and V are the mass density and the compressional wave velocity, respectively. Subscripts 1 and 2 denote media 1 and 2. The incident wave normal to the interface produces the transmitted and reflected wave in the same and opposite directions, respectively. For an obliquely incident wave, however, the multiple scattered waves are created and propagated according to the relation known as Snell's' law.

4.2 Measurement system

A pair of ultrasonic transducers was used to obtain the image by the ultrasonic wave reflection method, as shown in Fig. 4. The transducers transform mechanical waves into electrical signals and vice versa. For the proper selection of the ultrasonic transducer, the natural frequency, resolution, and directivity should be considered. A transducer with a natural frequency of 500 kHz was selected by considering the resolution and attenuation (Lee and Santamarina 2005, Lee *et al.* 2009, Troung *et al.* 2010). It should be noted that low-frequency waves generate images with low axial resolution but are less attenuated than high-frequency waves. In addition, focal-type transducers, which narrow the angle of beam, were used for high lateral resolution and amplification of the reflected waves. An aluminum foil-type shield around the transducer was used to minimize multiple reflections (Lee and Santamarina 2005, Lee *et al.* 2009, Troung *et al.* 2010).

A pulser (JSR Ultrasonics, DPR 300) was used to excite the source transducer, which generates an impulse signal. The ultrasonic waves produced from the source transducer propagated through the water and the lightly cemented soils. Then, the reflected waves at the interface were detected
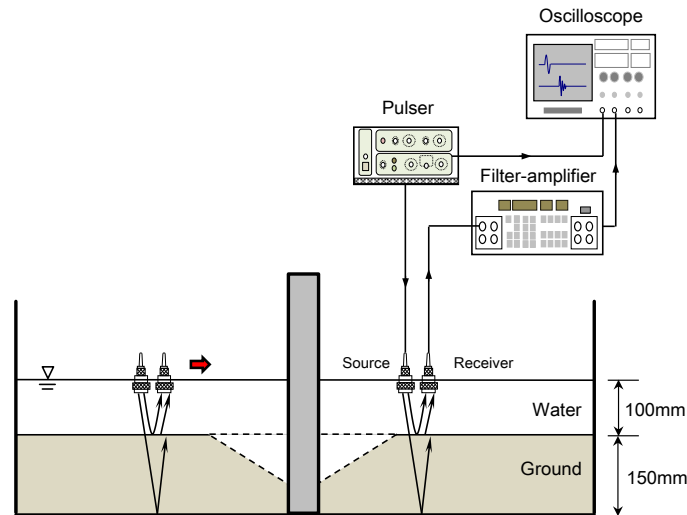
Fig. 4 Measurement system for a dynamic response using a strain gauge

by using the other transducer as a receiver. Using a filter and amplifier (Krohn-Hite 3945), the detected signals were amplified and filtered with a frequency range of 170 Hz to 26.5 MHz to remove the high frequency noise. The transducers were moved by using a horizontal scanning system, which has a scanning length of 400 mm and a scanning interval of 1.5 mm in the horizontal direction.

4.3 Test results

The ultrasonic reflection imaging was used to investigate the scour extent and shape near the model monopile. The reflected waves were measured by the ultrasonic transducers at scour depths of 0, 110, and 130 mm. The measured signal at scour depths of 0 mm is plotted in Fig. 5(a). For a better detection of the interface between the water and the specimen, an amplification factor was applied to the measured signals (Fig. 5(b)). Then, the negative component of the signals was converted to a positive value (rectification), as shown in Fig. 5(c), to change the signals to a suitable form in the imaging process. The signal was smoothed by using a moving average for the reduction of the high-frequency noise as shown in Fig. 5(d). Based on the results of previous studies (Zagzebski 1996, Lee *et al*. 2009), the signals with an amplitude less than 20% of the maximum amplitude were removed to filter the noise. The results of signal processing show that the reflected wave includes a strong reflection at the interface between the water and the specimen and a weak reflection at the bottom of the specimen.

The ultrasonic reflection images can be represented by these signals processed through amplification, rectification, moving average, and rejection. The ultrasonic reflection images of the scour according to the variance in the scour depth are represented in Fig. 6. In Fig. 6, two types of display methods were used: amplitude mode and brightness mode. In the amplitude mode and brightness mode, the ultrasonic reflection images clearly showed the scour shape and depth due to the impedance mismatch between the lightly cemented soils and water.
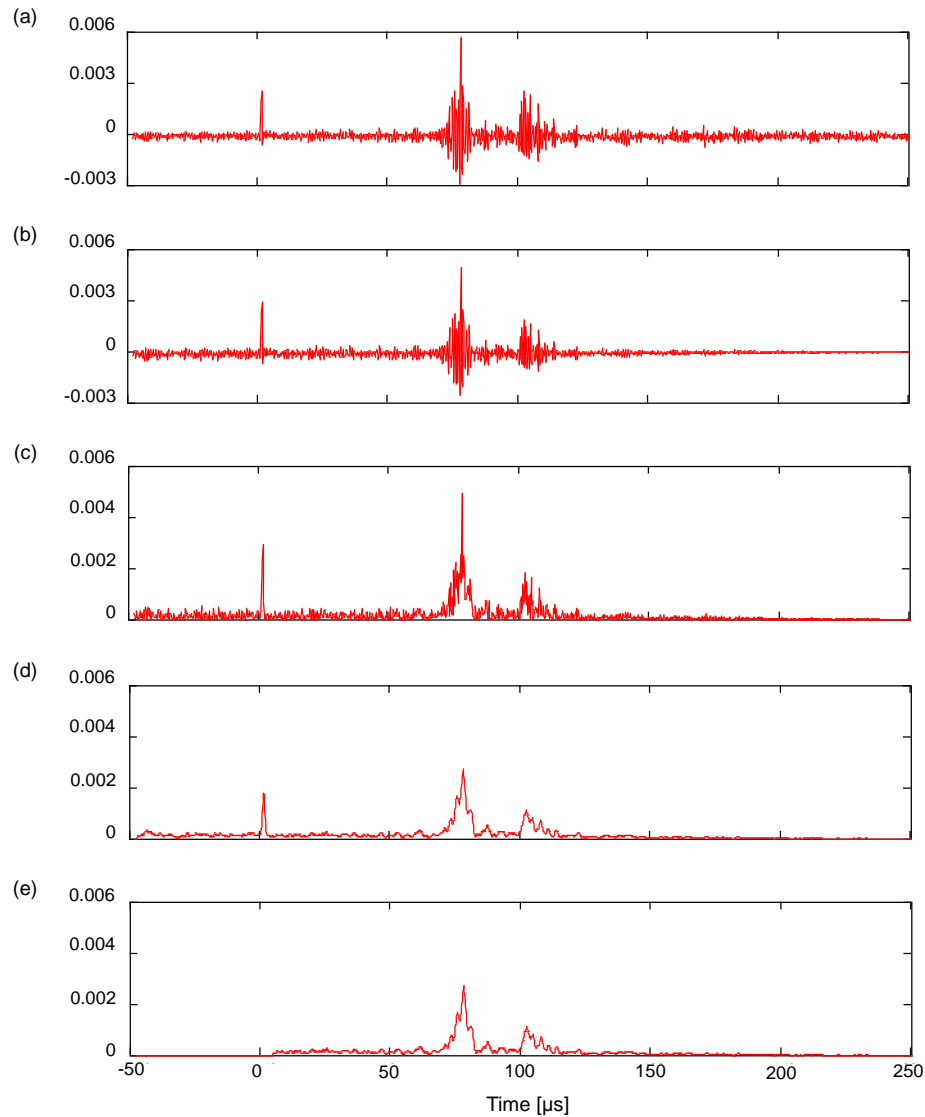
Fig. 5 Signal processing: (a) measured signal, (b) amplified signal, (c) rectification, (d) moving average and (e) rejection

5. Electrical resistivity profiling

5.1 Principle

The electrical conductivity of soils is used to estimate the soil properties, such as water content and void ratio. The electrical conductivity of saturated soils is composed of the electrical

conductivity of the soil particles, the electrical conductivity of the double layer, and the electrical conductivity of the electrolyte. In an offshore environment, the electrical conductivity of the electrolyte is significantly greater than those of the soil particles and double layer. Thus, the electrical conductivity of the seabed soils is mainly dependent on the concentration and distribution of electrolyte. Note that the electrical conductivity is the reciprocal of electrical resistivity. According to Archie's law (Archie 1942), the electrical resistivity of saturated soils (ρ_s) can be determined by the electrical resistivity of the pore water (ρ_w) as follows.

$$\rho_s = \alpha n^{-m} \rho_w \tag{4}$$

where *n* is the porosity of a soil. α and m are empirical constants, which are dependent on the tortuosity and soil type, respectively (Kim *et al.* 2011a).
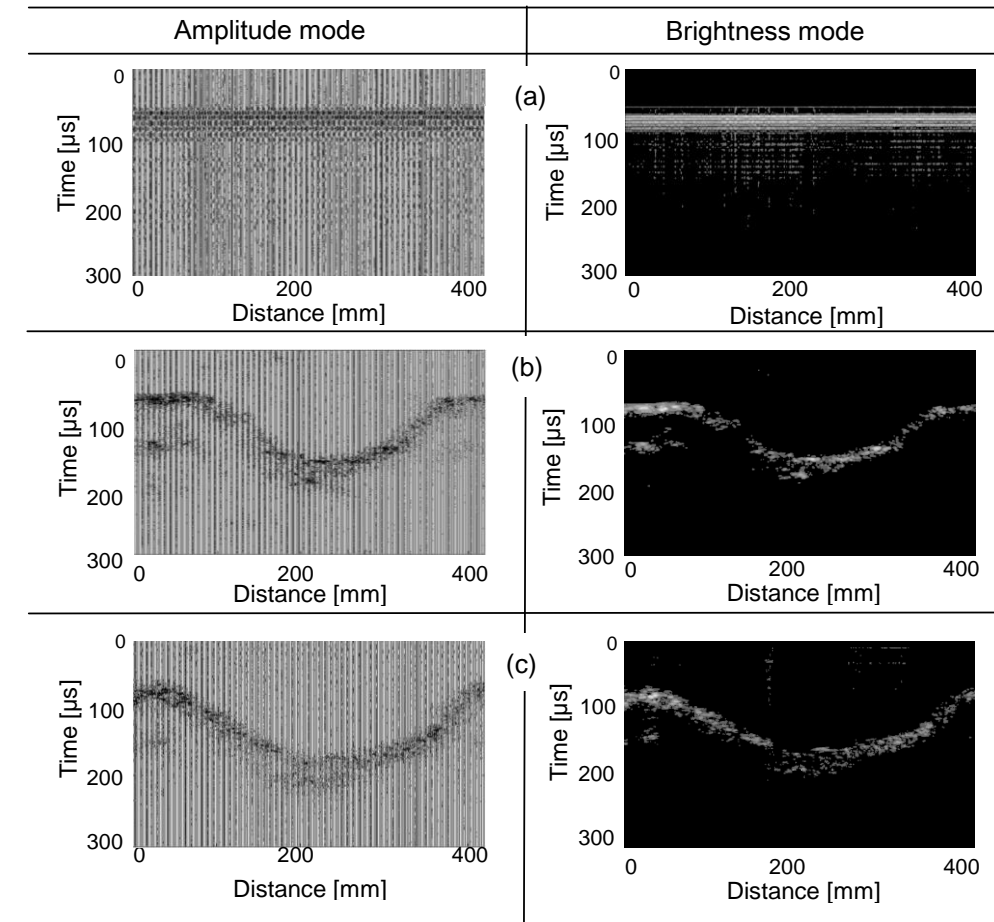

Fig. 6 Compressional wave scanning images according to scour depth: (a) 0 mm, (b) 110 mm and (c) 130 mm

5.2 Measurement system

The electrical resistivity of the lightly cemented soils adjacent to the model monopile was monitored by using a series of electrodes and an LCR meter, as shown in Fig. 7. For the electrical resistivity survey, a total of ten electrodes, each of which have a diameter of 3 mm, were installed on the surface of model pile at intervals of 30 mm in the vertical direction, as shown in Fig. 7. Two adjacent electrodes were connected to a four-terminal pair LCR meter (Intec LCR-819) with four coaxial cables. The four-terminal pair configuration is effective in reducing electrode polarization. In the connection configuration, one of the electrodes is used for high current (H_c) and high potential (H_p). The other electrode is used for low current (L_c) and low potential (L_p). To reduce electrical interference, the shield mesh of each of four coaxial cables was electrically connected with the others.

Electrical resonance in the electrodes connected with the cables may occur at particular resonance frequencies. To monitor the electrical resistance without the electrical resonance, frequency sweeping tests were carried out for the determination of operating frequency (Kim *et al*. 2011b). A low-frequency impedance analyzer (HP4192A), which can measure electrical resistance at a frequency range of 10 Hz–10 MHz, was used for frequency sweeping. For several salt waters with conductivities of 10, 20, 30, and 40 mS/cm, frequency sweeping tests were carried out from 100 Hz to 100 kHz, and the test results are plotted in Fig. 8. Fig. 8 shows that the electrical resistance measured by an electrode pair remained almost constant approximately 10 kHz. Therefore, the operating frequency of an electrode pair was set to be 10 kHz.
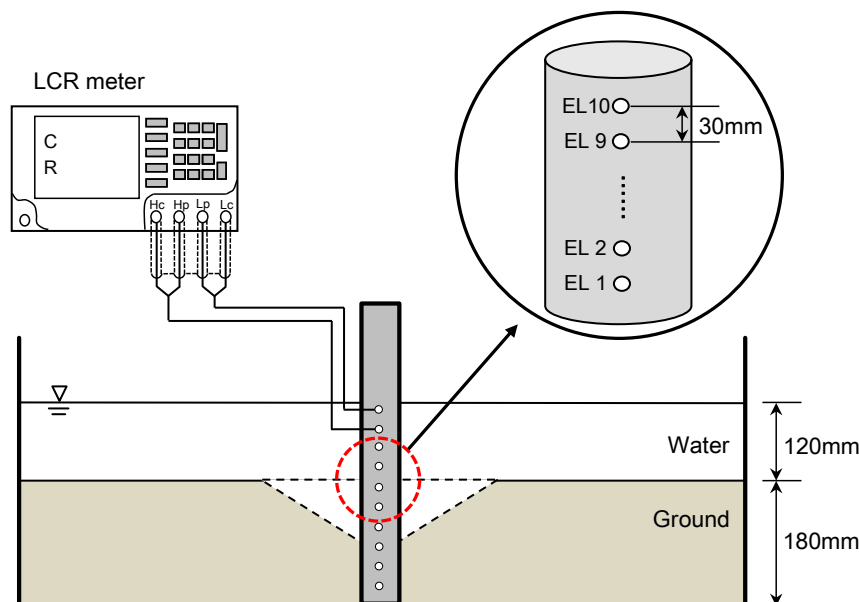

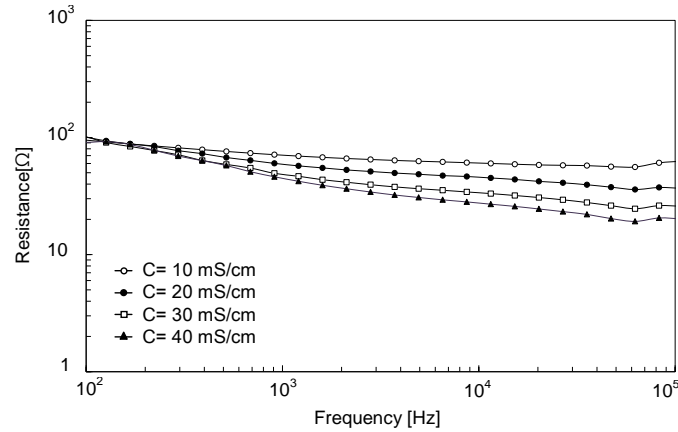Fig. 7 Measurement system for ultrasonic reflection imaging using transducers. EL denotes the electrodes

Fig. 8 Frequency sweeping as a function of the electrical conductivity. C denotes the conductivity of salt water

5.3 Test results

The electrical resistance measured by an electrode pair is dependent on the geometry and material properties of the electrodes. Thus, the measured electrical resistance should be converted into the electrical resistivity of the soil, which is independent of the characteristics of the electrodes (Lee *et al*. 2008, Yoon *et al*. 2011). Fig. 9 shows the relationship between the electrical resistance and the electrical resistivity in salt water with different electrical conductivities of 10, 20, 30, 40, and 50 mS/cm. From the results obtained by a pair of electrodes at the depth of 135 mm, the slope of the relationship between the electrical resistance and the electrical resistivity is 0.0055 m (see Fig. 9).
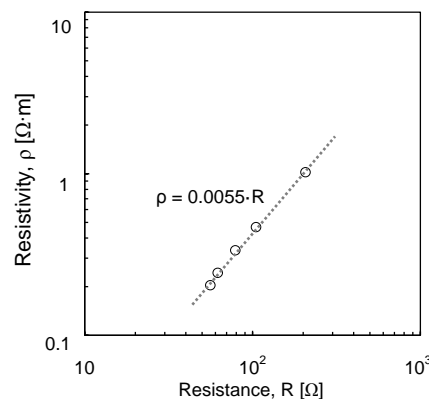
Fig. 9 Calibration of electrical resistivity using a pair of electrodes installed at a depth of 135 mm
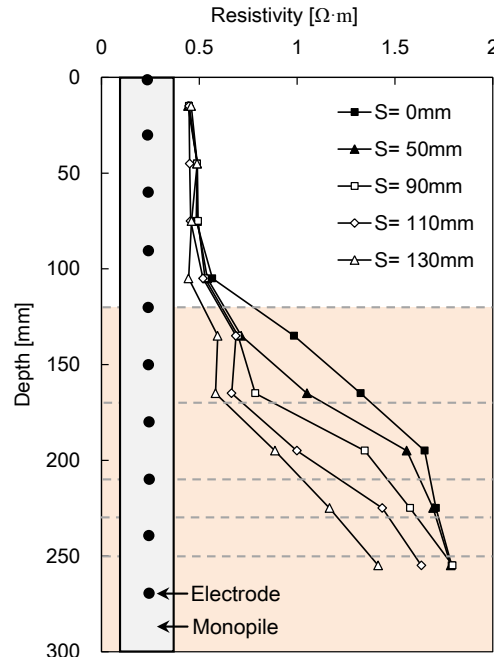
Fig. 10 Profiles of electrical resistivity according to scour depth. S denotes the scour depth

The electrical resistances measured at each electrode pair were converted into the corresponding electrical resistivities. The profiles of the electrical resistivity at scour depths of 0, 50, 90, 110 and 130 mm are plotted in Fig. 10. For modeling the offshore environment, the electrical conductivity of salt water was considered to be a constant 32 mS/cm. Fig. 10 shows that the electrical resistivity from the depth of 0 mm to 120 mm was approximately 0.5 $\Omega \cdot$m because the salt concentration in the water remains constant. For depths between 120 mm and 250 mm, the electrical resistivity increases with an increase in depth, while the electrical resistivity decreases with an increase in scour depth. Then, the electrical resistivity measured at the electrode pair gradually converged to 1.8 $\Omega \cdot$m. Note that the electrical resistivity values measured at the electrode pair completely embedded in the lightly cemented soils were greater than 1.3 $\Omega \cdot$m.

5. Discussion

The natural frequency of the monopile, the scour shape, and the scour depth were monitored by using the strain gauge, ultrasonic transducers, and electrodes. The variation of the natural period, which is the reciprocal of the natural frequency, along the scour depth is plotted in Fig. 11(a). The natural period of the monopile is proportional to the scour depth. The result shows that the increase of scour depth leads to an increase in the pile length and the natural period of the monopile. Thus, the scour depth can be estimated by monitoring the natural frequency using a strain gauge attached to the monopole.
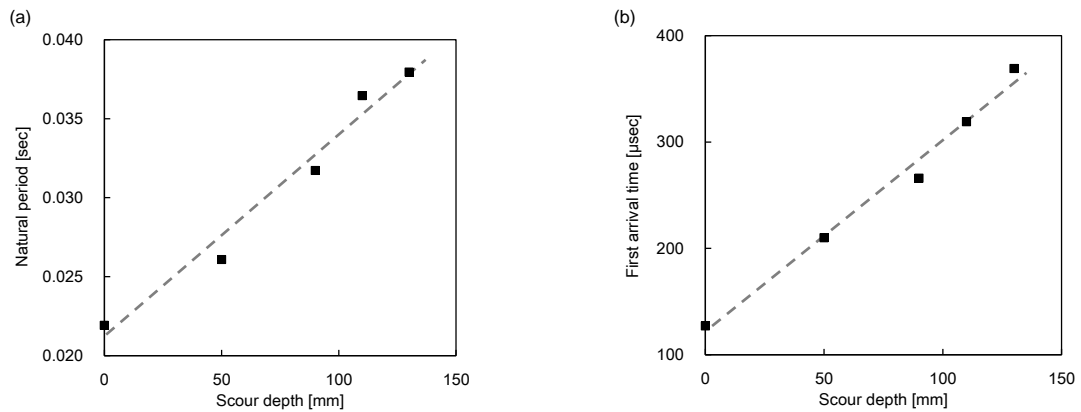
Fig. 11 Relationships among the first arrival time, natural period, and scour depth
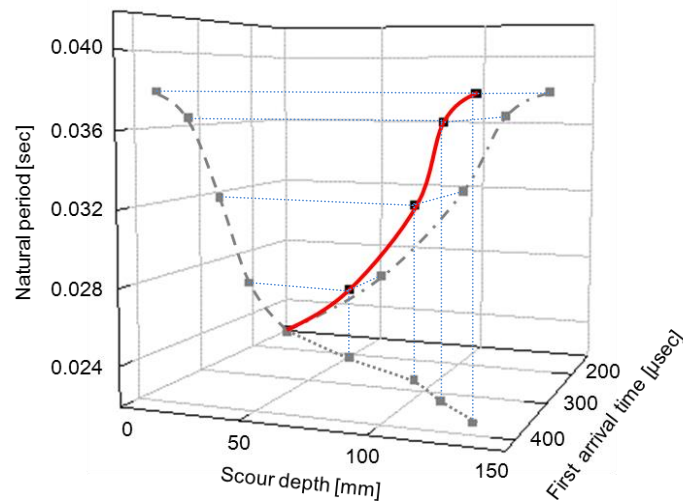

Fig. 12 Relationships among the first arrival time, natural period, and scour depth

*Solid line: 3D relationship,   dotted line: first arrival time v.s scour depth,
  dash-dotted line: natural period v.s scour depth,   dashed line: natural period v.s first arrival tim

A compressional wave, which propagates with a constant wave velocity in a given medium, can be used to estimate the scour shape and scour depth by checking the first arrival of the reflected waves. Fig. 11(b) shows that the first arrival time increases with an increase in the scour depth. In addition, according to the scour depth, the relationship between the first arrival time of the reflected wave and the natural period of the monopile is plotted in Fig. 12. Overall, the natural period of the monopile and the first arrival time increases with an increase in the scour depth.

Consequently, the results demonstrate that ultrasonic reflection imaging accompanied with natural frequency measurement may be useful for monitoring the scour depth and scour shape.

The electrical resistivity measured by each electrode pair as a fixed monitoring instrument was used for the estimation of the local scour depth. The electrical resistivity measured at the electrode pairs ranged from 0.5 Ω·m to 1.8 Ω·m, as shown in Fig. 10. The minimum and maximum electrical resistivity corresponded to the values in salt water and in deep soils, respectively. Note that the porosity of the deep soils may be smaller than that of the surface soils. In addition, the water and surface soils may not be clearly discriminated by the value of electrical resistivity because of the wide sensing range of the electrode pair in the model monopile. To more accurately assess the local scour depth, the sensing distance of the electrode pair and the porosity of the soils should be considered (Kim *et al*. 2011a, b). Moreover, in this study, the ratio of salt water and deep soils remained between two electrodes affects the variation in the electrical resistivity profile. However, considering that the scour depth developed in the field is on the order of meters, the resolution of the electrode pair with intervals of 30 mm is high enough to accurately detect the local scour depth.

6. Conclusions

The scour around the monopile foundation was evaluated by using three different monitoring techniques: (a) natural frequency measurement; (b) ultrasonic reflection imaging; and (c) electrical resistivity profiling. For the physical model test, the lab-scale monopile and geo-materials were prepared in a cylindrical tank. First, the natural frequency measurement was carried out by using a strain gauge attached to the monopile. Second, the ultrasonic waves reflected at the interface between two media were monitored by ultrasonic transducers. Finally, the local scour depth was detected by a series of electrodes mounted on the monopile. The model tests with each monitoring techniques were carried out as functions of the scour depth.

Dynamic strain signals in time domain obtained from the strain gauge were converted into frequency domain to determine the natural frequency of the model monopile. The natural frequency of the model monopile decreased with an increase in the scour depth. The ultrasonic reflection images obtained after signal processing clearly detected the scour shape and scour depth. The results demonstrated that the first arrival of the reflected ultrasonic waves increased with an increase in the scour depth. The electrical resistivity increased with an increase in depth and decreased with an increase in scour depth. The results of electrical resistivity profiles showed that for more accurate evaluation of the scour depth, the sensing distance of electrode pair, porosity of soils, and the ratio of salt water and deep soils between two electrodes should be considered. In this study, the techniques using the strain gauge, ultrasonic transducers, and electrodes as fixed instruments may be effectively used for the scour monitoring of offshore monopile foundations.

Acknowledgments

References

Andersen, L.V., Vahdatirad, M.J., Sichani, M.T. and Sørensen, J.D. (2012), "Natural frequencies of wind turbines on monopile foundations in clayey soils—A probabilistic approach", *Comput. Geotech.*, **43**, 1-11.

Andrews, D. and Bennett, A. (1981), "Measurements of diffusivity near the sediment-water interface with a fine-scale resistivity probe", *Geochim. Cosmochim. Ac.*, **45**(11), 2169-2175.

Archie, G.E. (1942), *The Electrical Resistance Log as an Aid in Determining Some Reservoir Characteristics*. I. Pet Tech, 5.

Babu, M.R., Sundar, V. and Rao, S.N. (2003), "Measurement of scour in cohesive soils around a vertical pile-simplified instrumentation and regression analysis", *IEEE J. Ocean. Eng.*, **28**(1), 106-116.

Briaud, J.L., Medina-Cetina, Z., Hurlebaus, S., Everett, M., Tucker, S., Yousefpour, N. and Arjwech, R. (2012), *Unknown foundation determination for scour* (No. FHWA/TX-12/0-6604-1).

Cooper, T., Chen, H., Lyn, D., Rao, A. and Altschaeffl, A. (2000), *A Field Study of Scour Monitoring Devices for Indiana Streams*, Joint Transportation Research Program, **2**.

Den Boon, J.H., Sutherland, J., Whitehouse, R., Soulsby, R., Stam, C.J.M., Verhoeven, K. and Hald, T. (2004), "Scour behaviour and scour protection for monopile foundations of offshore wind turbines", *Proceedings of the European Wind Energy Conference*, **14**.

De Vries, P., Burges, S.J., Daigneau, J. and Stearns, D. (2001), "Measurement of the temporal progression of scour in a pool-riffle sequence in a gravel bed stream using an electronic scour monitor", *Water Resour. Res.*, **37**(11), 2805-2816.

Kim, J.H., Yoon, H.K., Cho, S.H., Kim, Y.S. and Lee, J.S. (2011a), "Four electrode resistivity probe for porosity evaluation", *Geotech. Test. J. ASTM*, **34**(6), 668-675.

Kim, J.H., Yoon, H.K. and Lee, J.S. (2011b), "Void Ratio Estimation of Soft Soils using Electrical Resistivity Cone Probe", *J. Geotech. Geoenviron.*, **137**(1), 86-93.

Lee, C., Lee, J.S., Lee, W. and Cho, T.H. (2008), "Experiment Setup for Shear Wave and Electrical Resistance Measurements in an Oedometer", *Geotech. Test. J. ASTM*, **31**(2), 149-156.

Lee, I.M., Truong, Q.H., Kim, D.H. and Lee, J.S. (2009), "Discontinuity detection ahead of a tunnel face utilizing ultrasonic reflection : Laboratory scale application", *Tunn. Undergr. Space Technol.*, **24**(2), 155-163.

Lee, J.S. and Santamarina, J.C. (2005), "P-wave reflection imaging", *Geotech. Test. J. ASTM*, **28**(2), 197-206.

Lin, Y.B., Lai, J.S., Chang, K.C. and Li, L.S. (2006), "Flood scour monitoring system using fiber bragg grating sensors", *Smart Mater. Struct.*, **15**, 1950-1959.

Meirovitch, L. (1967) Analytical methods in vibrations.

Nawa, R.K. and Frissell, C.A. (1993), "Measuring scour and fill of gravel streambeds with scour chains and sliding-bead monitors", *North Am. J. Fish Manage.*, **13**(3), 634-639.

Qi, W.G. and Gao, F.P. (2014), "Physical modeling of local scour development around a large-diameter monopile in combined waves and current", *Coast. Eng.*, **83**, 72-81.

Truong, Q.H., Lee, C., Cho, G.C. and Lee, J.S. (2010), "Geophysical monitoring techniques for underwater landslide in 1g models", *J. Environ. Eng. Geophys.*, **15**(1), 1-19.

Whitehouse, R. (2006), "Scour at Coastal Structures", *Proceedings of International Conference on Scour and Erosion 2006*.

Whitehouse, R., Harris, J., Sutherland, J. and Rees, J. (2008), "An assessment of field data for scour at offshore wind turbine foundations", *4th International Conference on Scour and Erosion in Tokyo on November 2008*, HR Wallingford, 1-8.

Yoon, H.K., Jung, S.H. and Lee, J.S. (2011), "Characterization of Subsurface Spatial Variability by Cone Resistivity Penetrometer", *Soil Dyn. Earthq. Eng.*, **31**(7), 1064-1071.

Zagzebski, J.A. (1996), *Essentials of Ultrasound Physics*. Mosby Inc., Missouri.

Zanke, U.C., Hsu, T.W., Roland, A., Link, O. and Diab, R. (2011), "Equilibrium scour depths around piles in noncohesive sediments under currents and waves", *Coast. Eng.*, **58**(10), 986-991.

Zhao, M., Cheng, L. and Zang, Z. (2010), "Experimental and numerical investigation of local scour around a submerged vertical circular cylinder in steady currents", *Coast. Eng.*, **57**(8), 709-721.

Zhou, Z., Huang, M., Huang, L., Ou, J. and Chen, Genda. (2011), "An optical fiber grating sensing system for scour monitoring", *Adv. Struct. Eng.*, **14**(1), 67-78.

CC